Available online at www.sciencedirect.com
ScienceDirect
Trans. Nonferrous Met. Soc. China 28(2018) 1538−1542
Transactions of Nonferrous Metals Society of China
www.tnmsc.cn

Atomic scale structural characterization of $\{10\bar{1}2\}$ twin boundaries in zinc

Hai-chen WU, You-xing YU, Xiao-fang BI

School of Materials Science and Engineering, Beihang University, Beijing 100191, China

Received 18 May 2017; accepted 10 November 2017

Abstract: The structure and the migration mechanisms of $\{10\bar{1}2\}$ twin boundaries (TBs) of pure zinc deformed by rolling were studied using high-resolution transmission electron microscopy (HRTEM) at atomic scale. We found the presence of basal/prismatic (BP/PB) planes serrations on $\{10\bar{1}2\}$ TBs and the coexistence of two kinds of TBs with different structures in the same $\{10\bar{1}2\}$ twin: TBs composed of $\{10\bar{1}2\}$ coherent twin boundaries (CTBs) plus short BP/PB serrations, and TBs composed of successive BP/PB segments without $\{10\bar{1}2\}$ CTBs. The formation of BP/PB serrations has no relation to the *c*/*a* ratio of hexagonal-close-packed (HCP) metals because the BP/PB serrations are energetically preferred and geometrically favored. Based on dislocation theory, we proposed the migration mechanisms of the TBs to be the glide of twinning dislocations (TDs) on the CTBs and the climb of interface dislocations (IDs) on the BP/PB segments.

Key words: zinc; twin boundaries; basal/prismatic BP/PB serrations; migration mechanism; high-resolution transmission electron microscopy (HRTEM)

1 Introduction

Deformation twinning plays a critical role in plastic deformation of metals with hexagonal-close-packed (HCP) structure because of insufficient number of available slip systems. In comparison to metals with cubic structures, the twinning modes in HCP metals are more complex, and different twinning modes including $\{10\bar{1}n\}$ and $\{11\bar{2}n\}$ (n=1, 2, 3, 4) could be activated when the metal is subjected to different mechanical loading modes [1]. Of the various twinning modes, the $\{10\bar{1}2\}$ mode is the most commonly activated one. As a consequence, the nucleation, propagation and growth mechanisms of $\{10\bar{1}2\}$ twin have been given much attention both experimentally and theoretically in recent years [2−5]. The propagation of $\{10\bar{1}2\}$ twin has been ascribed to the successive glide of twinning dislocations or disconnections (TDs) with a step height of two atomic layers on $\{10\bar{1}2\}$ twinning planes, and atomic shuffling is also required to move all the atoms to the correct twin positions in addition to glide [1,6−8]. Since the early studies, the $\{10\bar{1}2\}$ twin boundaries (TBs) have been observed to exhibit abnormal characteristics, i.e., the macroscopic TB can deviate significantly from the crystallographic $\{10\bar{1}2\}$ twinning plane, and the misorientation relation between matrix and twin can also deviate largely from the ideal twin misorientation relation [9−11]. Recent experimental observations in magnesium and cobalt at atomic scale [4,5,9−11] suggested that these deviations could be attributed to the unique structure of $\{10\bar{1}2\}$ TBs, which is composed of $\{10\bar{1}2\}$ coherent twin boundaries (CTBs) together with basal-prismatic planes serrations (PBs and BPs). The BP or PB serrations are specific steps on TBs with the geometrical characteristic of the basal plane of the matrix parallel to the prismatic plane of the twin, or vice versa [12,13]. The BP/PB serrations have been observed in HCP metals (Mg [4,8,10,12], Co [9] and Ti [14,15]) with $\gamma<\sqrt{3}$ (γ is the *c*/*a* ratio), where formation of $\{10\bar{1}2\}$ twins will generate a tension strain along the *c*-axis. However, for HCP metals with $\gamma>\sqrt{3}$, where formation of $\{10\bar{1}2\}$ twins will generate a compression strain along the *c*-axis, the BP/PB serrations have not been observed yet. In this work, we reported experimental observation of $\{10\bar{1}2\}$ TBs in zinc (with the *c*/*a* ratio of 1.856) at atomic scale using high resolution transmission election microscopy (HRTEM). We found the presence of BP/PB serrations on $\{10\bar{1}2\}$ TBs and the coexistence of two kinds of TBs with different structures in the same $\{10\bar{1}2\}$ twin: TBs composed of $\{10\bar{1}2\}$ CTBs plus short BP/PB serrations, and TBs composed of

Corresponding author: You-xing YU; Tel: +86-10-82315999; E-mail: yuyouxing@buaa.edu.cn
BI Xiao-fang; Tel: +86-10-82339231; E-mail: bixf@buaa.edu.cn
DOI: 10.1016/S1003-6326(18)64749-1

successive BP/PB segments without $\{10\bar{1}2\}$ CTBs. Then, we proposed the migration mechanisms of these TBs based on dislocation theory.

2 Experimental

Polycrystalline pure Zn (purity 99.99%) was deformed by rolling to a total reduction of 50% in thickness by three passes at room temperature. The rolled samples were prepared for TEM characterization by double-jet electrolytic polishing at −25 °C in electrolyte consisting of 6% perchloric acid and 94% alcohol. HRTEM observations were carried out using a JEM2100F electron microscope operated at 200 kV. The detailed boundary characterization was conducted on a Titan G2 60−300 Cs-corrected electron microscope operated at 300 kV.

3 Results

Figure 1 shows a typical TEM micrograph of a long grain boundary indicated by white arrows after rolling deformation. The inserted selected area electron diffraction (SAED) patterns taken from a large range across the grain boundary demonstrate that the two grains have a perfect $\{10\bar{1}2\}$ twin orientation relation, indicating the long grain boundary to be $\{10\bar{1}2\}$ TB. The trace of the $\{10\bar{1}2\}$ twinning plane is marked by a yellow line in the matrix and by a green line in the twin according to the SAED patterns. Intriguingly, the TB exhibits different characteristics at different positions. On the upper side, the TB exhibits a relatively straight morphology, and is parallel to the trace of the $\{10\bar{1}2\}$ twinning plane. While on the left side, the TB shows a curved morphology, and deviates significantly from the $\{10\bar{1}2\}$ twinning plane. The deviation angle between the actual TB and the $\{10\bar{1}2\}$ twinning plane can reach 90° at some positions. This large deviation from the theoretical twinning plane exceeds the deviation usually observed on the tips of lenticular twins [1], which can be attributed to the presence of regularly arranged twinning dislocations on the incoherent TB.

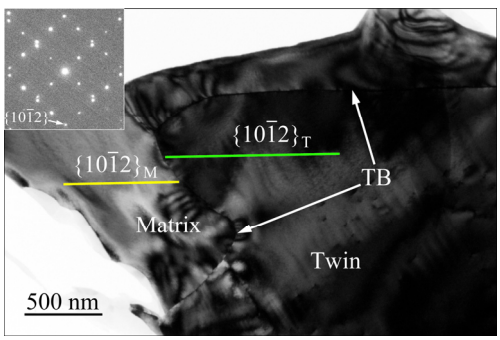

Fig. 1 TEM micrograph of $\{10\bar{1}2\}$ twin boundary and corresponding SAED pattern

In order to clarify the microstructure of the $\{10\bar{1}2\}$ TB at atomic scale, HRTEM analyses were conducted. Figure 2 shows the HRTEM image of the upper side of the above $\{10\bar{1}2\}$ TB. It is obvious that the TB is composed of $\{10\bar{1}2\}$ CTBs connected by short BP and PB serrations. The misorientation angle between the matrix and the twin is measured to be about 86° according to the traces of the basal planes, approximately equal to the ideal value (86.3°) of $\{10\bar{1}2\}$ twin orientation relation, indicating that the $\{10\bar{1}2\}$ twin orientation relation still maintains well despite the presence of the BP/PB serrations. The inserted SAED patterns taken from this region also confirm an evident $\{10\bar{1}2\}$ twin orientation relation.

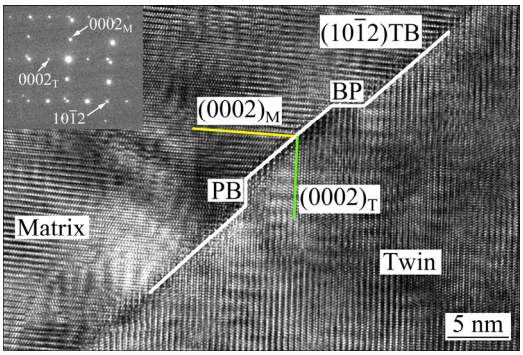

Fig. 2 HRTEM image and corresponding SAED pattern of coherent twin boundary

The HRTEM image of the left side of the above TB is shown in Fig. 3. The inserted SAED patterns taken from this region demonstrate a definite $\{10\bar{1}2\}$ twin orientation relation, the same as in Fig. 2. However, attention should be paid to the fact that the TB here exhibits incoherent characteristic and does not coincide with any well defined crystallographic planes. The trace of the $\{10\bar{1}2\}$ twinning plane is marked by a yellow line in the matrix and by a green line in the twin according to the SAED patterns. Obviously, the actual TB deviates significantly from the theoretical $\{10\bar{1}2\}$ twinning plane. The deviation angle between the actual TB and the $\{10\bar{1}2\}$ twinning plane can vary in a large range, from nearly 50° to 90°. The misorientation angle between the matrix and the twin is measured to be still about 86°, very close to the ideal value (86.3°), suggesting that the significant deviation from the theoretical $\{10\bar{1}2\}$ twinning plane and the breakdown of the coherency of the TB do not break the $\{10\bar{1}2\}$ twin orientation relation. To throw light on the detailed structure of the incoherent TB, a Cs-corrected HRTEM image is provided in Fig. 4. It can be observed that the incoherent TB is composed of successive BP and PB segments perpendicular to each other, as indicated by blue lines, without the participant of $\{10\bar{1}2\}$ CTBs. This

unique structure can give rise to the curved configuration of the actual TB deviating largely from the theoretical $\{10\bar{1}2\}$ twinning plane, because the successive BP/PB segments can form a macroscopic boundary of any shape by containing BP/PB steps with different lengths and proportions.

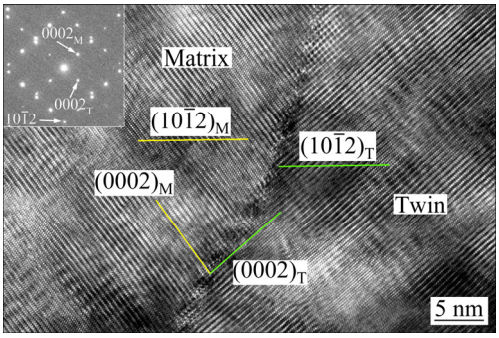

Fig. 3 HRTEM image and corresponding SAED pattern of incoherent twin boundary

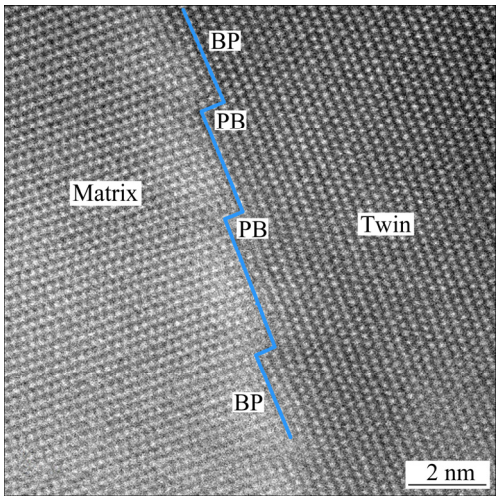

Fig. 4 Cs-corrected HRTEM image of incoherent twin boundary

4 Discussion

According to the above observations, we can make the following conclusions: 1) the BP/ PB serrations could exist on $\{10\bar{1}2\}$ TBs of zinc with the *c*/*a* ratio larger than $\sqrt{3}$; 2) two kinds of TBs with different structures, i.e., TBs composed of $\{10\bar{1}2\}$ CTBs connected by short BP/PB serrations (referred to as serrated CTBs in the following) and TBs composed of successive BP/PB segments without the presence of $\{10\bar{1}2\}$ CTBs, could coexist in the same $\{10\bar{1}2\}$ twin; 3) the $\{10\bar{1}2\}$ twin orientation relation maintains well throughout the whole region, despite the presence of the BP/PB serrations or the large deviation of the actual TB from the theoretical $\{10\bar{1}2\}$ twinning plane. Based on these, two questions could be raised: 1) Does the *c*/*a* ratio of a certain HCP metal have any effect on the presence of BP/PB serrations on twin boundary? and 2) how do the two kinds of TBs migrate?

For the first question, the BP/PB serrations have already been universally observed in Mg, Co and Ti with the *c*/*a* ratio less than $\sqrt{3}$ both experimentally and theoretically. Combined with our present observations, we can conclude that the formation of BP/PB serrations has no relation to the *c*/*a* ratio. Atomistic simulations show that the formation of BP/PB serrations is energetically preferred and geometrically favored [16−18]. During plastic deformation, dislocation slip is usually activated accompanied by deformation twinning. Lattice dislocations can dissociate on CTBs, and interact with CTBs or transmit across CTBs to the adjacent grain. In addition, CTBs can also serve as nucleation sources of lattice dislocations that glide away from CTBs. In all cases, residual defects will be left on the CTBs, resulting in the CTBs exhibiting serrated configurations or the misorientation angle between matrix and twin deviating from the ideal twin orientation relation. During further deformation, BP or PB serrations can form on the CTBs as a result of accumulation of these residual defects within the CTBs, leading to reduction of the excess energy of the dislocated CTBs. Energy calculations show that the BP/PB serrations have a relatively low formation energy (170 mJ/m^2) which is comparable to the formation energy of CTBs (122 mJ/m^2) [16], meaning that the BP/PB serrations are thermodynamically stable. Thus, formation of BP/PB serrations is energetically preferred.

Furthermore, according to the geometrical characteristic of $\{10\bar{1}2\}$ twin, the misorientation angle between the basal planes of the matrix and the twin is nearly 90° across the twin boundary. In other words, the basal plane of the matrix is nearly parallel to the prismatic plane of the twin, or vice versa. This geometrical relationship nearly coincides with the geometrical characteristic of BP/PB serrations, where the basal plane of one grain is parallel to the prismatic plane of the other. This means that the BP/PB serrations are geometrically favored. In the present case of zinc, the exact $\{10\bar{1}2\}$ twin orientation relation is not disrupted by the presence of BP/PB serrations, even the absence of $\{10\bar{1}2\}$ CTBs has no influence on the twin orientation relation. Since the actual misorientation angle between the matrix and the twin is 86.3° rather than 90°, geometrically necessary grain boundary dislocations should be present on the TBs to accommodate the nearly 4° of misorientation angle. It is the presence of grain boundary dislocations, which contributes to keeping the $\{10\bar{1}2\}$ twin orientation relation well, otherwise the actual misorientation relation may deviate from the ideal twin orientation relation, as observed in Mg and Co [4,5,9−11].

Then, we proposed the probable migration mechanisms of the two kinds of TBs. For the serrated CTBs (Fig. 5(a)), TDs dipoles with the Burgers vector of $b_{tw}=(3-\gamma^2)/(3+\gamma^2)[10\bar{1}1]$ ($\gamma=c/a$) [1,6] first nucleate and glide along the $\{10\bar{1}2\}$ CTBs, leading to the migration of CTBs. These TDs are of glide-shuffle type with a step height of two atomic layers. As for the BP/PB serrations, recent topological modeling and MD simulations [16,18] revealed that the migration of BP/PB serrations could be accomplished via the climb of interface dislocations (IDs) along the BP/PB serrations with the magnitude of Burgers vector to be $|b_{ID}|=-(\sqrt{3}-\gamma)a$. The IDs are also two atomic layers thick and are of climb-shuffle type. When the gliding TDs meet the BP/PB serrations, they will be impeded. Then, the TDs can dissociate into IDs that climb on the BP/PB serrations, leading to the BP/PB serrations migration. The migration of the BP/PB serrations means the transformation between the basal planes and the prismatic planes of the matrix and the twin, which depends on the c/a ratio and the stress state. For zinc with $\gamma>\sqrt{3}$, the basal planes will transform into the prismatic planes when the BP/PB serrations are subjected to a compression stress, while the prismatic planes will transform into the basal planes when the BP/PB serrations are subjected to a tension stress. Due to the difference in the interplanar spacing between the basal planes and the prismatic planes, the critical stress needed to activate the IDs between compression and tension is also different. When the CTB is subjected to a shear stress, there will be a normal stress component perpendicular to the BP/PB serrations since the BP/PB serrations deviate nearly 45° with respect to the CTB. The shear stress will drive the nucleation and glide of TDs along the CTBs, while the normal stress will drive the dissociation of TDs into IDs and the climb of IDs along the BP/PB serrations, cooperatively accomplishing the migration of the serrated CTBs, as indicated by green arrows in Fig. 5(a).

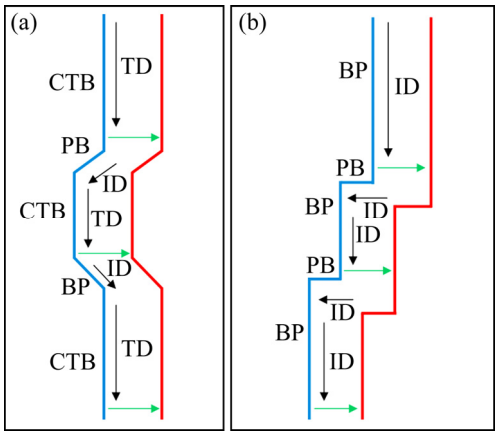

Fig. 5 Mechanisms of twin boundaries migration: (a) Coherent twin boundary; (b) Incoherent twin boundary

For the TB consisting of successive BP/PB segments (Fig. 5(b)), it can be deemed as an extreme case where the length of CTBs shrinks to zero. As a result, the successive BP/PB segments will migrate only via the climb of IDs while TDs are not involved. Since the IDs cannot form via the dissociation of TDs, the IDs must nucleate directly on the BP/PB segments under a relatively high normal stress. According to the geometrical characteristic of the entire $\{10\bar{1}2\}$ twin (Fig. 1), when the serrated CTB on the upper side is subjected to a shear stress, there will be normal stress components on the successive BP/PB segments on the left side. When the normal stress on the BP/PB segments reaches the critical value, nucleation of IDs of climb-shuffle type could be activated. Then, the migration of the incoherent TB will be accomplished via the cooperative climb of IDs on the perpendicularly successive BP/PB segments, as indicated by green arrows in Fig. 5(b).

Combining above analyses, the migration of the TB is accomplished via the glide of TDs on the CTBs and the climb of IDs on the BP/PB segments. Because the nucleation and glide of TDs along the CTBs could be activated under a relatively low shear stress, the migration of the incoherent TB composed of successive BP/PB segments is more difficult than the serrated CTBs. As the BP/PB segments can serve as effective obstacles of TDs glide, increasing the density and the height of the BP/PB segments will significantly impede the migration of TBs, and correspondingly hinder the deformation process related to twinning, which will improve the mechanical strength of HCP metals.

5 Conclusions

1) Two kinds of TBs with different structures could coexist on $\{10\bar{1}2\}$ twin boundaries of rolling deformed zinc: TBs composed of $\{10\bar{1}2\}$ CTBs plus short BP/PB serrations, and TBs composed of successive BP/PB segments without $\{10\bar{1}2\}$ CTBs.

2) The formation of BP/PB serrations has no relation to the c/a ratio of HCP metals because the BP/PB serrations are energetically preferred and geometrically favored.

3) The migration mechanisms of the TBs can be deduced as the glide of TDs on the CTBs and the climb of IDs on the BP/PB segments.

References

[1] CHRISTIAN J W, MAHAJAN S. Deformation twinning [J]. Progress in Materials Science, 1995, 39: 1−157.

[2] HAN Ting-zhuang, HUANG Guang-sheng, WANG You-gen, WANG Guan-gang, ZHAO Yan-chun, PAN Fu-sheng. Microstructure and formability evolutions of AZ31 magnesium alloy sheets undergoing

continuous bending process [J]. Transactions of Nonferrous Metals Society of China, 2016, 26: 2043−2050.
[3] LUAN Bai-feng, YE Qing, CHEN Jian-wei, YU Hong-bing, ZHOU Dong-li, XIN Yun-chang. Deformation twinning and textural evolution of pure zirconium during rolling at low temperature [J]. Transactions of Nonferrous Metals Society of China, 2013, 23: 2890−2895.
[4] LIU Bo-yu, WANG Jian, LI Bin, LU Lu, ZHANG Xi-yan, SHAN Zhi-wei, LI Ju, JIA Chun-lin, SUN Jun, MA E. Twinning-like lattice reorientation without a crystallographic twinning plane [J]. Nature Communications, 2014, 5: 3297.
[5] LI Bin, ZHANG Xi-yan. Global strain generated by shuffling-dominated $(10\bar{1}2)\langle 10\bar{1}1\rangle$ twinning [J]. Scripta Materialia, 2014, 71: 45−48.
[6] THOMPSON N, MILLARD D J. Twin formation in cadmium [J]. Philosophical Magazine, 1952, 43(339): 422−440.
[7] LI B, MA E. Atomic shuffling dominated mechanism for deformation twinning in magnesium [J]. Physical Review Letters, 2009, 103(3): 035503−035506.
[8] OSTAPOVETS A, MOLN ÀR P. On the relationship between the “shuffling-dominant” and “shear-dominant” mechanisms for $\{10\bar{1}2\}$ twinning in magnesium [J]. Scripta Materialia, 2013, 69: 287−290.
[9] ZHANG X Y, LI B, TU J, SUN Q, LIU Q. Non-classical twinning behavior in dynamically deformed cobalt [J]. Materials Research Letters, 2015, 3(3): 142−148.
[10] LIU Bo-yu, WAN Liang, WANG Jian, MA E, SHAN Zhi-wei. Terrace-like morphology of the boundary created through basal-prismatic transformation in magnesium [J]. Scripta Materialia, 2015, 100: 86−89.
[11] LI Bin, ZHANG Xi-yan. Twinning with zero twinning shear [J]. Scripta Materialia, 2016, 125: 73−79.
[12] XU B, CAPOLUNGO L, RODNEY D. On the importance of prismatic/basal interfaces in the growth of $(\bar{1}012)$ twins in hexagonal close packed crystals [J]. Scripta Materialia, 2013, 68(11): 901−904.
[13] OSTAPOVETS A, BURŠÍK J, GRÖGER R. Deformation due to migration of faceted $\{10\bar{1}2\}$ twin boundaries in magnesium and cobalt [J]. Philosophical Magazine, 2015, 95(36): 4106−4117.
[14] LI Y J, CHEN Y J, WALMSLEY J C, MATHINSEN R H, DUMOULIN S, ROVEN H J. Faceted interfacial structure of $\{10\bar{1}1\}$ twins in Ti deformed during equal channel angular pressing [J]. Scripta Materialia, 2010, 62(7): 443−446.
[15] KIM I, KIM J, SHIN D H, LIAO X Z, ZHU Y T. Deformation twins in pure titanium processed by equal channel angular pressing [J]. Scripta Materialia, 2003, 48(6): 813−817.
[16] WANG J, LIU L, TOMÉ C N, MAO S X, GONG S K. Twinning and de-twinning via glide and climb of twinning dislocations along serrated coherent twin boundaries in hexagonal-close-packed metals [J]. Materials Research Letters, 2013, 1(2): 81−88.
[17] WANG J, BEYERLEIN I J. Atomic structures of symmetric tilt grain boundaries in hexagonal close packed (hcp) crystals [J]. Modelling and Simulation in Materials Science and Engineering, 2012, 20(2): 1−22.
[18] WANG J, YADAV S K, HIRTH J P, TOMÉ C N, BEYERLEIN I J. Pure-shuffle nucleation of deformation twins in hexagonal-close-packed metals [J]. Materials Research Letters, 2013, 1(3): 126−132.

原子尺度下纯锌中$\{10\bar{1}2\}$孪晶界的结构表征

吴海辰，俞有幸，毕晓昉

北京航空航天大学 材料科学与工程学院，北京 100191

摘 要：通过高分辨透射电子显微镜研究原子尺度下轧制变形后的纯锌中$\{10\bar{1}2\}$孪晶界的结构和迁移机制，发现在$\{10\bar{1}2\}$孪晶界上存在基面/柱面锯齿，并且在同一个$\{10\bar{1}2\}$孪晶中存在两种结构不同的孪晶界：由$\{10\bar{1}2\}$共格孪晶界和微小基面/柱面锯齿组成的孪晶界，以及由连续基面/柱面锯齿组成的不包含$\{10\bar{1}2\}$共格孪晶界的孪晶界。基面/柱面锯齿的形成与密排六方金属的轴比无关，因为基面/柱面锯齿的形成在能量上和几何上都是有利的。基于位错理论，孪晶界的迁移是由孪生位错在共格孪晶界上的滑移以及界面位错在基面/柱面锯齿上的攀移来实现的。

关键词：锌；孪晶界；基面/柱面锯齿；迁移机制；高分辨透射电镜

(Edited by Xiang-qun LI)